

Liquefaction Analysis of Beach Protection Structure: Numerical Simulations

Abdul Hakam^{#1}, Junaidi^{#2}, Bayu M Adji^{#3}, Shafira R Hape*, M Sofian Asmirza⁺

[#]Civil Engineering, Faculty of Engineering, Andalas University, Padang 25163, West of Sumatra, Indonesia
E-mail: ¹ahakam2008@yahoo.com; ²ahakam@ft.unand.ac.id; ³junaidi_joe@gmail.com; ^{*}bayumartantoadji@gmail.com

^{*}Gadjah Mada University, Yogyakarta, Indonesia
E-mail: shafirarahmadilla@gmail.com

⁺North Sumatra University, Medan, Indonesia
E-mail: sofyan0076@yahoo.co.uk

Abstract—The damage on infrastructures as well as environmental losses can be triggered by abrasion. That is why abrasion is included one kind of concerning disasters in Indonesia. West Sumatra is one of the provinces in Indonesia where its shoreline faces directly to the Indian Ocean. The West Sumatra shoreline abrasion phenomena have been recorded since earlier year 1900s. Abrasion prevention structures generally can be used to minimize the damage in near shore infrastructures. Cobblestone type groin is the most popular abrasion prevention structures to protect coastlines in the West Sumatra. West Sumatra groins were usually placed directly on the beach sand. The stability of the kind of groins is then greatly influenced by the mechanical state of the soil. Practically, the groins were designed in the static state which considers self-weight and the wave forces. In fact, due to dynamic forces the stability of the groins can be reduced. The external dynamic forces can increase in inertia forces and the change of the soil condition. Earthquake may lead the groins' base soil to liquefy which can disrupt the stability of the groins in terms of loss of bearing capacity. This study described the numerical simulation results to observe groin stability due to liquefaction. The liquefaction phenomena is simulated by increasing the applied pore pressure in the soil mass. The simulation results are then plotted in terms of shear-normal stress diagrams. The groin stability is then observed using the Mohr-Coulomb failure criterion. This study found that groin stability is not only disrupted by full liquefaction, but the liquefaction state can also disrupt the groin stability. It is also found that the groin dimensions affect the stability against a certain liquefaction level.

Keywords— liquefaction; abrasion protection structure; numerical analysis.

I. INTRODUCTION

Abrasion is the uncontrolled sea wave energy may cause kind of erosion along the shoreline. Abrasion can be involved as a part of the sediment transport process along the coastline. Due to abrasion, the shoreline may change in from its original in terms of accretion or secretion. Abrasion also may be worsened by the loss of natural protection on a beach, then the advantages of the marine plants must be elaborated to protect the beach [1]. There are many losses caused by abrasion in Indonesia to give a reason that the government includes this natural process into one disaster that needs to be managed [2]. The damage due to abrasion may be reduced by the wave energy breaker constructions on the shoreline or by eliminating sediment transport along the beach by ground cover methods.

Environmental losses along beaches due to abrasion become a matter of concern to researchers for decades. The abrasion along the coastline may be linked up to the global warming. Zhang et al. in 2004 [3] have concluded there are a relationship between the sea level rise due to the effects of global warming with the coastal damage that happened from the 19th to the 20th centuries. The study found there is about twice damage happened to the beaches with the rate of sea level rise. This study warns that the coastal abrasion problems induced by the global warming scenario may be worse in the 21st century. The beaches are placed where many [4] communities live and depend on. Then their preservation needs to be protected.

The damage to the coastal environment also may be caused by human activities on the land [5]. Then it will be again worsened by global warming [6]. Abrasion can also turn the beaches into critical condition as reported in

Malaysia [7]. The same condition also happens to the beaches along West Sumatra coastline caused by abrasion [8]. The abrasion protection actions are needed to prevent those beaches (Fig 1). The promising natural protection methods using marine plantations have been studied [9]. The other artificial beach rock made of sand solidification may be a prospect of beach environmental protection [10]. To

minimize the bad environmental effect, a suitable abrasion protection method which is human-made must be carefully chosen [11]. The use of hard structures for abrasion protection can reduce environmental values. So, further studies on the effects of abrasion protections to environmental are necessarily conducted.

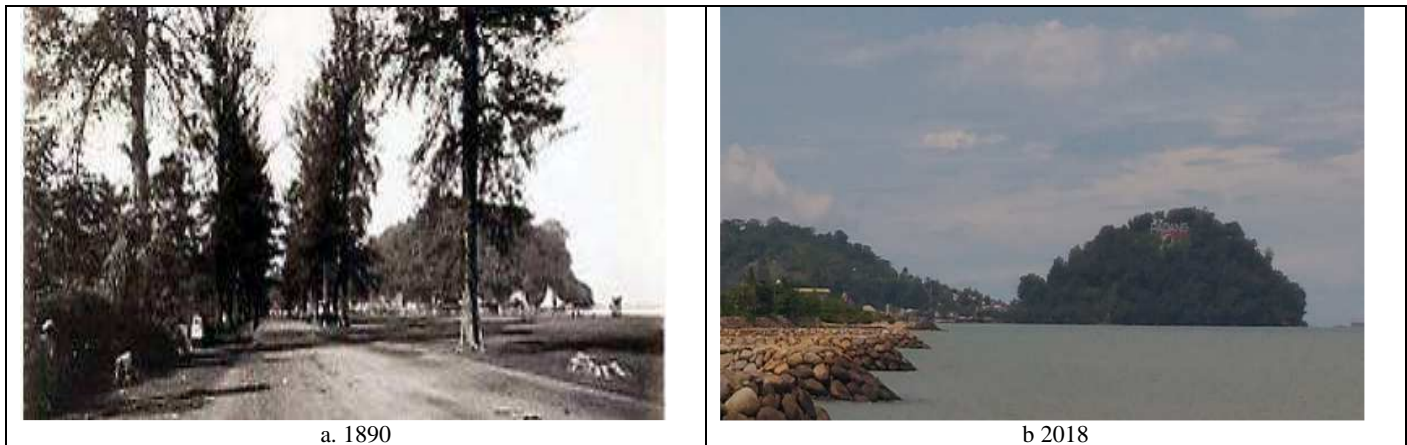


Fig 1. Padang beach in 1890 [13] and 2018

A recent study on the marine plantation for beaches protection along West Sumatra shoreline found that some endemic vegetation still exists. That vegetation can be classified as wave-resistant marine plantations. Those marine vegetation are sea pine, coconut, mangroves and locally trees called *pinago* and *ketaping* [12]. The computer modeling has also been done to show the mechanism of roots in protecting beaches. The numerical simulation reasonably presents the role of plantation roots to prevent the sandy beach taken away by seawater [1].

In West Sumatra, stone groin (groin) structures become the most popular abrasion prevention method to be chosen to protect coastlines. Groins are constructed by well arranging the original mountain stone on the beach sand. The stability of the groins is greatly influenced by the mechanical state of the underneath soil. An earthquake can lead to liquefaction to the base sands so that may disrupt the stability of the groins. This study presents the numerical simulation analyses to observe stability due to liquefaction.

II. MATERIAL AND METHOD

The previous study on beach abrasion protection has conducted field investigations to exploit the beach soil sediment along West Sumatra coastline. The laboratory tests of soil samples then were done to gain the physical properties of soils [12]. The beach soil sediments predominantly are coarse groin particles with less cohesive materials in them. There are seven soil samples had been tested from different locations along West Sumatra coastline. The laboratory test results are re-shown in Figure 2 below.

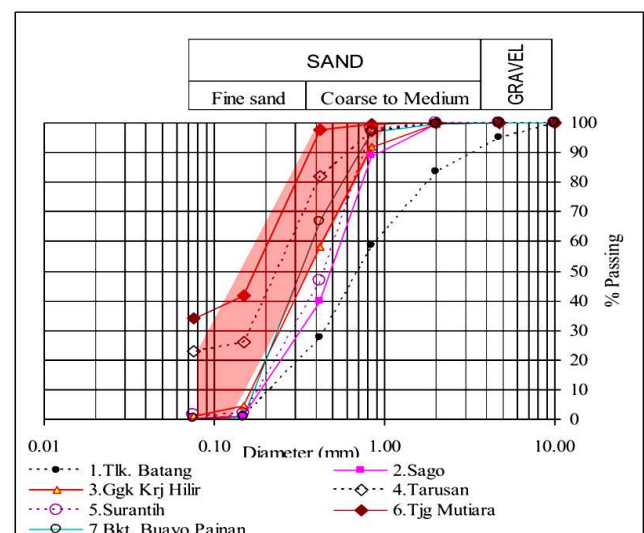


Fig 2. Beach sands in West Sumatra [12]

To find out the liquefaction potential in these soils, in Fig 2 is also plotted the area of limit liquefaction potential for sandy soils [14]. It can be seen the sands taken from two areas namely Tarusan and Tanjung Mutiara are very potential to liquefy. While the sand from Bukit Buayo Painan site also has the possibility of liquefaction potential as most of the gradation curves are within the limits of the liquefaction area. So, for the locations with liquefaction potential, the stability of the construction against liquefaction is necessary to be employed in the design of abrasion prevention constructions. In this study, a typical procedure to analyze the stability of the groin structure against liquefaction was presented.

The beach sand parameters for numerical modeling are taken from [1]. The strength parameters are adopted from a direct shear test with the internal friction angle of 32.3 degree and cohesive strength of 0.94 kN/m². The elasticity parameters are soil modulus of 52352 kN/m², Poisson's ratio is 0.25. The unit weights are 12.37 kN/m³ in 16.36 kN/m³ in dry and saturated conditions respectively.

Typical groin structure to be modeled in numerical simulations is adopted from the existing groins which have been made along the coast of Padang (Fig 3). The groins are made of mountain rock arrangement with a height dimension of about 5m, 5m of crest width and the side slope is 45

degrees. The other data to be used in the numerical analysis are 50 degrees for internal friction angle with a modulus of elasticity twice the ground sand.

In the numerical simulation, initially, the groin system was built and analyzed to obtain the stress distribution in the system. The same model then was executed with the increased pore pressure. The stresses in the pore water were increased to model the pore pressure due to liquefaction. The simulation was repeated with the higher applied pore pressure in the system. The total stress and effective stresses in the soil mass in the series simulation were recorded and plotted in the same graph.



Fig 3. Typical groin in West Sumatra

In the numerical simulation, initially, the groin system was built and analyzed to obtain the stress distribution in the system. The same model then was executed with the increased pore pressure. The stresses in the pore water were increased to model the pore pressure due to liquefaction. The simulation was repeated with the higher applied pore pressure in the system. The total stress and effective stresses in the soil mass in the series simulation were recorded and plotted in the same graph.

The stresses in the soil mass in any load condition can be written in the following relationship:

$$\sigma' = \sigma - u \quad (1)$$

where: σ' is the effective stress in the soil mass
 σ is the total stress, and
 u represents the pore pressure.

The shear and normal stresses at any points in the soil mass can be plotted in the same graph. Based on the obtained shear and normal stresses in the base soil mass, the stability of the groin can be analyzed. Mohr-Coulomb's failure criterion is then used to investigate the stability of the analyzed groin system. The failure envelope of this criterion is expressed with the straight line which represents shear-normal stress relationship in failure condition (Fig 4). Shear-normal stress pairs at any points which are under the failure line indicate the stable condition of those points. On the other hand for any points above the line indicate the failure condition of the points. The straight failure line in the shear-normal stress relationship is written as:

$$\tau' = c + \sigma' \tan \phi \quad (2)$$

where: τ' is the shear effective stress
 σ' is the normal effective stress
 ϕ is internal friction angle, and
 c is the soil cohesion

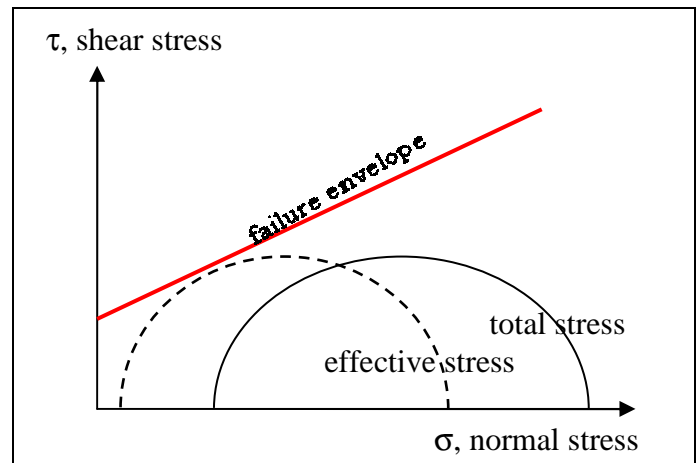


Fig 4. Shear-normal stress relationship

III. RESULTS AND DISCUSSION

Simulation to illustrate the effect of liquefaction to groin stability is using the numerical model. The base soil and groin materials are modeled to follow the Mohr-Coulomb constitutive law. The series of numerical simulation is then performed with several stages as follows:

- Original conditions where there is no groin.
- Initial conditions at the time groin are built.
- The condition with the increased pore water pressure.

The original condition is performed to calculate the initial stresses in the soil mass due to the self-weight of the base

soil as well as hydrostatic pore pressure. The initial state is representing the model after the construction of groin as shown in Fig 5. The typical numerical results in terms of stresses are shown in Fig 6 for pore water pressure, for. 7 for total stress and Fig 8 for effective stress..

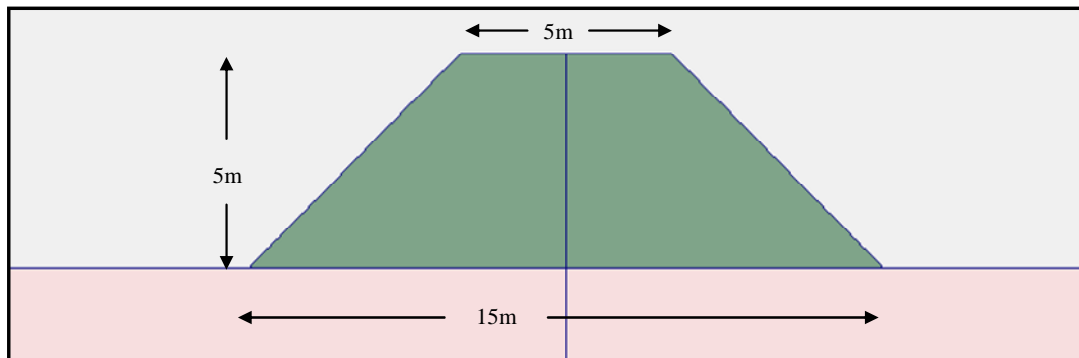


Fig 5. The numerical model of the groin

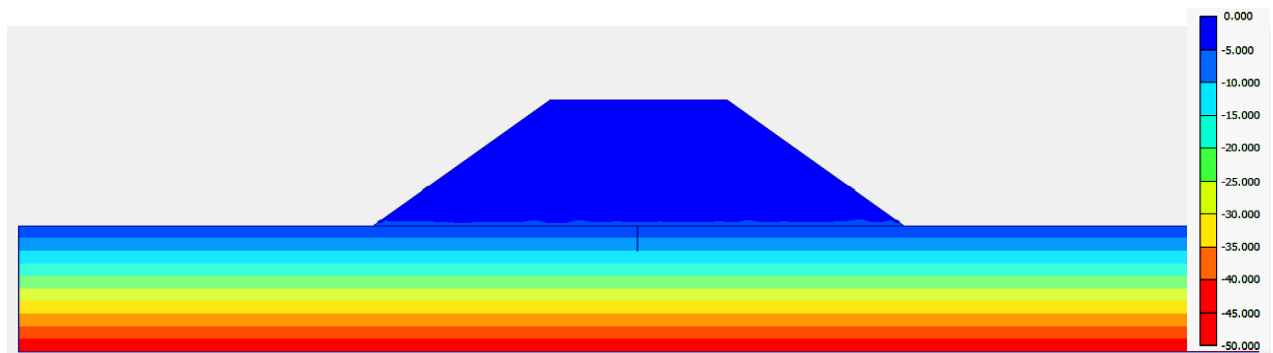


Fig 6. The pore water pressure

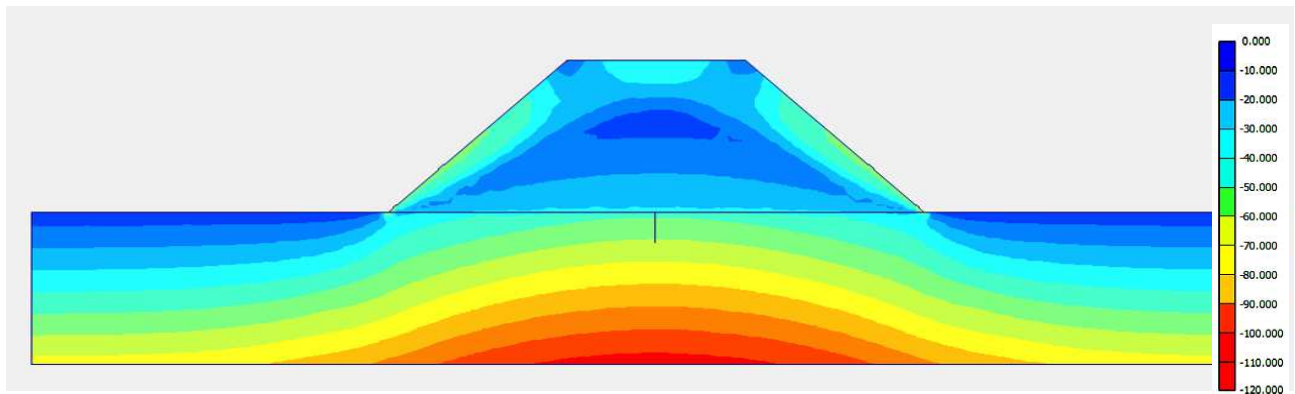


Fig 7. The total stress

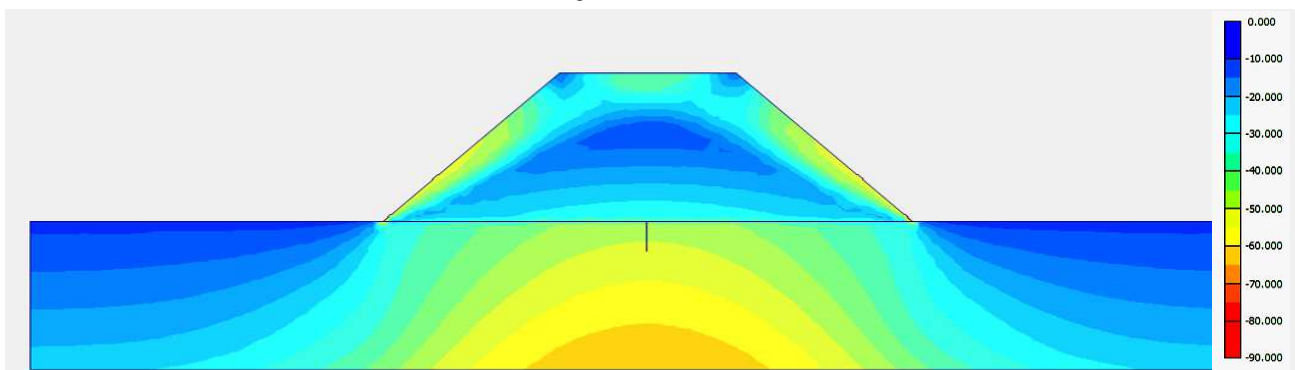


Fig 8. Effective stress

In the original condition, where there is no groin building thereon, it is required as an initial reference to determine the stress values in the original soil mass. These specified stresses are used to describe the stress position of the soil in the Mohr-Coulomb diagram. Furthermore, the condition at the beginning of the groin construction is necessary to describe the stress values caused by the additional self-weight of the groin structure. Then the initial condition is executed to analyze the initial stresses in the soil mass before the increased pore water pressure exists. In this simulation, the highlights for drawing the Mohr's Circle (Fig 9) are taken under the groin center.

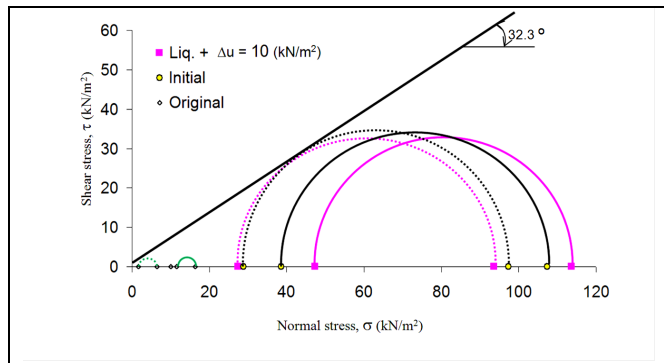


Fig 9. Mohr's circle for the stresses in the soil mass

Then, the minor and major stresses can represent horizontal and vertical stress as well. While the next conditions where the increased pore water pressure has been existing, are to describe the stresses due to liquefaction. The stresses drawn in Mohr's circle are determined at a depth of 1 m from the middle-bottom of the groin structure, that are dotted and straight circles for effective and total stresses respectively. The results of numerical calculation on the original condition are presented in terms of the total and effective stresses. The values of the stresses at a 1-meter depth are 16.4 kN/m² and 11.6 kN/m² in the vertical direction and horizontal direction respectively. These values are total major and minor principal stresses on initial conditions. The pore pressure at this initial state is as big as 10 kN/m² in all directions that implies the stresses of 6.4 and 1.6 for major and minor principal stresses. Those stress values are drawn in terms of Mohr's Circles in the green colors. It can be seen that the effective stress circle is still under the failure envelope.

At the initiative of the groin construction, the total principal stresses that occur at point 1m below the groin are 107.3 kN/m² and 38.6 kN/m² for major and minor respectively. While effective stresses at the same point are 97.4 kN/m² and 28.8 kN/m² for major and minor respectively. In this initial condition, the safety factor of the groin is 1.20. This safety factor generally provides a fairly good value against static loads. This condition presents the relatively safe of the groin designed. However, it can be seen that the effective Mohr's Circle in this initial state is closed to the failure line. It indicates that the groin stability will be easily disturbed by the additional external or internal forces.

In the event of liquefaction, there will be an increase in pore water stress in the soil. The increased stress is

simulated by providing pore-water pressure corresponding to a multiplication of as much as twice of a static state. The principal effective stresses at point 1m below the groin are 93.7 kN/m² and 27.4 kN/m² for major and minor respectively. These stresses are drawn in the graph with the red colors. It can be seen that the total stress in the soil is increased meanwhile its effective stress is reduced. At this state, the safety factor of the groin is reduced until 1.12 which is lower than its original one.

In this simulation, the zero effective stresses will not be reached for any calculations. The main reason is the groin construction will completely collapse before the zero effective stress is reached. It can be illustrated using the Mohr's Circles in Fig 10 with three circles names Circle-1, Circle-2, and Circle-3. Let assume that all three circle are representing the effective stresses in the saturated soil mass. The Circle-1 is representing the safe condition where all of stress in the soil is still under the failure envelope. When the pore pressure in the soil mass is increased, the effective stress will be reduced, and at the critical condition, it will shift to Circle-2. The Circle-2 is exactly touched the failure line. If then the pore pressure is further increased, the stresses in the soil mass will produce the Circle-3. This circle is crossing the failure line in two points. This condition, of course, will not happen since the soil mass has been collapse before it. Then, for zero or negative effective stresses in the soil mass may not happen theoretically. But, in fact, it may happen in terms of the sand boil or mass flow phenomena.

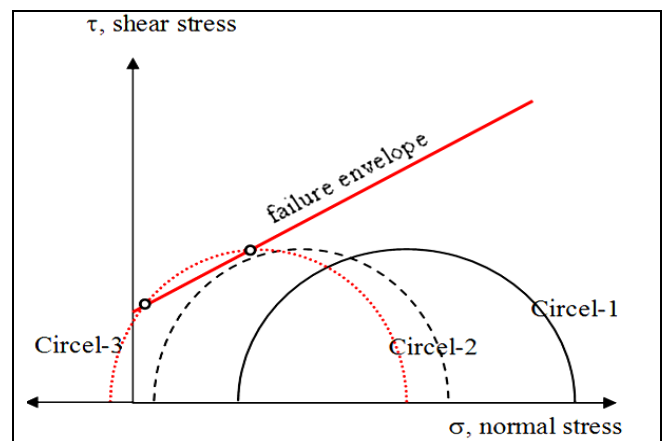


Fig 10. Zero effective stress illustration

IV. CONCLUSION

The beach abrasion is one disaster that has resulted in infrastructures and environmental losses in Indonesia. To reduce the abrasion effect in West Sumatra has been provided abrasion prevention structures in terms of the groin. Since the groins were directly constructed on the beach sand, then their stability is greatly influenced by the mechanical state of the soil. The increased pore water pressure due to liquefaction may reduce the groin's stability. That phenomenon has been elaborated using numerical simulation in this study. It has been shown event at incomplete liquefaction state, the stability of groin in term of safety factor can be reduced. Then it is necessary to predict the

stability of groin that may collapse due to earthquake induced liquefaction.

ACKNOWLEDGMENT

The authors would like to acknowledge the faculty of engineering, Andalas University, Padang, West Sumatra, Indonesia (No. Contract 002/UN.16.09 D/PL/2018) for funding the publication of this article.

REFERENCES

- [1] A. Hakam, B. Istijono, and T. Ophiyandri, "Vegetations as Beach Protection: Simulations of Root Protection Mechanism Against Abrasion," *Int. J. Adv. Sci. Eng. Inf. Technol.*, vol. 7, no. 6, p. 2316, Dec. 2017.
- [2] National Disaster Management Plan, "The Regulation of the Head of National Disaster Management Agency No. 07/2012: Guidelines for Data Management and Disaster Information in Indonesia (Peraturan Kepala Badan Nasional Penanggulangan Bencana No. 07/2012: Pedoman Pengelolaan Data dan Informasi)," Jakarta, 2012.
- [3] K. Zhang, B. C. Douglas, and S. P. Leatherman, "Global Warming and Coastal Erosion," *Clim. Change*, vol. 64, no. 1/2, pp. 41–58, May 2004.
- [4] E. Arthur B, F. Vladimir R, and L. Ma. Teresa B, "Socio-Ecological and Livelihood Assessment of Selected Coastal Areas in Sorsogon, Philippines," *Int. J. Adv. Sci. Eng. Inf. Technol.*, vol. 5, no. 4, p. 339, 2015.
- [5] Y. W. Soedarto, L. Hanum, and M. S. Lestari, "Analysis and Identification of Landuse on the Coastal Environment of South Sumatra using GIS," *Int. J. Adv. Sci. Eng. Inf. Technol.*, vol. 7, no. 3, p. 785, Jun. 2017.
- [6] D. Yuliadi, - Eriyatno, M. Y. J. Purwanto, and I. W. Nurjana, "Socio Economical Impact Analysis and Adaptation Strategy for Coastal Flooding (Case Study on North Jakarta Region)," *Int. J. Adv. Sci. Eng. Inf. Technol.*, vol. 6, no. 3, May 2016.
- [7] Balai Wilayah Sungai Sumatera (BWSS) V, "Identification of Critical Coast in West Sumatera Province (Identifikasi Pantai Kritis di Propinsi Sumatera Barat)," Padang, 2009.
- [8] M. A. Othman, "Value of mangroves in coastal protection," *Hydrobiologia*, vol. 285, no. 1–3, pp. 277–282, Jun. 1994.
- [9] R. A. Feagin *et al.*, "Going with the flow or against the groin? The promise of vegetation for protecting beaches, dunes, and barrier islands from erosion," *Front. Ecol. Environ.*, vol. 13, no. 4, pp. 203–210, May 2015.
- [10] M. N. Hasan Khan, "Artificial Beachrock Formation Through Sand Solidification Towards the Inhibit of Coastal Erosion in Bangladesh," *Int. J. Geomate*, vol. 9, no. 2, pp. 1528–1533, 2016.
- [11] J. E. Dugan, D. M. Hubbard, I. F. Rodil, D. L. Revell, and S. Schroeter, "Ecological effects of coastal armoring on sandy beaches," *Mar. Ecol.*, vol. 29, no. s1, pp. 160–170, Jul. 2008.
- [12] B. Istijono, A. Hakam, and T. Ophiyandri, "Investigation of The Effects of Plant Variety and Soil Sediment to The Coastal Abrasion in West Sumatra," *Int. J. GEOMATE*, vol. 14, no. 44, pp. 52–57, 2018.
- [13] Ohgihito, "Minangkabau Tempo Doeloe #1 - Padang," 2012. [Online]. http://ohgituto.blogspot.com/2012/11/minangkabau-tempo-doeloe-1_27.html.
- [14] A. Hakam, "Laboratory Liquefaction Test of Sand Based on Groin Size and Relative Density," *J. Eng. Technol. Sci.*, vol. 48, no. 3, pp. 334–344, 2016.